

Reduction of train-induced vibrations on adjacent buildings

Hsiao-Hui Hung[†], Jenny Kuo[†] and Yeong-Bin Yang[‡]

Department of Civil Engineering, National Taiwan University, Taipei, Taiwan, R.O.C.

Abstract. In this paper, the procedure for deriving an infinite element that is compatible with the quadrilateral Q8 element is first summarized. Enhanced by a self mesh-expansion procedure for generating the impedance matrices of different frequencies for the region extending to infinity, the infinite element is used to simulate the far field of the soil-structure system. The structure considered here is of the box type and the soils are either homogeneous or resting on a bedrock. Using the finite/infinite element approach, a parametric study is conducted to investigate the effect of open and in-filled trenches in reducing the structural vibration caused by a train passing nearby, which is simulated as a harmonic line load. The key parameters that dominate the performance of wave barriers in reducing the structural vibrations are identified. The results presented herein serve as a useful guideline for the design of open and in-filled trenches concerning wave reduction.

Key words: finite/infinite element method; in-filled trench; infinite element; open trench; traffic-induced vibration; wave barrier.

1. Introduction

As the high-technology community enters the so called “age of nanometer”, the traffic-induced vibration in buildings or factories becomes an issue of great concern. Most highly developed cities or metropolises in the world have encountered the problem that transportation constructions inevitably come across or close to vibration-sensitive residential or industrial areas. Micro-vibrations, which though may not result in collapse of structures as earthquakes do, have been known to cause architectural damages and malfunction of delicate instruments located inside the buildings. In highly vibration-sensitive applications, it is of critical importance that the major vibration sources be identified, analyzed and isolated, when necessary, as part of the facility design process.

The ground-borne vibration due to the railway traffic has been a subject of increasing research in recent years due to the construction of highspeed railways worldwide. In general, research on this subject can be classified into four categories. The first relates to design of special track systems as a first aid to mitigate the transmission of vibration directly generated by the trains. Elaborate vehicle-track interaction models have been used in this regard. For instance, the floating slab track (Grootenhuis 1977, Wilson *et al.* 1983, Balendra *et al.* 1989), which consists of concrete slab track supported on resilient elements, has been proved to be a very effective measure for isolating the vibration at frequencies above the resonance frequency of the floating slab system. The second is to

[†] Formerly Graduate Student

[‡] Professor

investigate the influence of train speed on ground vibration and to investigate the propagation of vehicle-induced vibrations via the soils to areas alongside of the railways. Both theoretical methods with the assumption of elastic homogenous soils and experimental investigations have been employed in this regard (Gutowski and Dym 1976, Dawn and Stanworth 1979, Alabi 1992, Krylov and Ferguson 1994, Krylov 1995, Heckl *et al.* 1996, Madshus *et al.* 1996). The third category is focused on the design of buildings to mitigate the traffic-induced vibrations. For instance, theoretical solutions were obtained by Takahashi (1985, 1986a, b) using the plate elements to simulate a box-type structure subjected to a harmonic line force on the surface of a viscoelastic half space under different boundary conditions, where an optimal choice of the structure thickness and material was proposed based on a parametric study. The last category is concerned with the installation of various wave barriers, such as open and in-filled trenches (Woods 1968, Lysmer and Wass 1972, Segol *et al.* 1978, Emad and Manolis 1985, Beskos 1986, Al-Hussaini and Ahmad 1991, 1996, Ahmad *et al.* 1996, Yang and Hung 1997), buried concrete plates (Schmid *et al.* 1991, Antes and von Estorff 1994), or aligned piles (Boroomand and Kaynia 1991), between the railways and the buildings to be protected. These barriers are not only helpful for isolating the vibration caused by the passing trains, but also for reducing ground-transmitted waves generated by other vibration sources, such as machines, vehicles, blasting, etc. In this paper, only the fourth category will be dealt with.

Concerning the wave isolation of structures from ground-borne vibrations, a great volume of research has been conducted in the past using analytical or experimental methods. In early studies employing analytical approaches, restrictions were often imposed on the geometry and material properties of the problem considered, as close-form solutions cannot be easily obtained for complex conditions. On the other hand, although the results obtained by the experimental methods appear to be most reliable and close to real situations, an exhausted field test may cost a lot. Starting from the mid 1970s, various numerical methods emerged as effective tools for solving the wave propagation problems. By the lumped mass method, Lysmer and Wass (1972) studied the effectiveness of a trench in reducing the horizontal shear wave motion induced by a harmonic load acting on the rigid footing lying on the horizontal layer. Segol *et al.* (1978) used finite elements, along with special non-reflecting boundary, to investigate the isolation efficiency of open and bentonite-slurry-filled trenches in layered soils. The axisymmetric infinite elements that are capable of dealing with multiple wave components have been employed by Yang and Yun (1992) and Yun and Kim (1995) to deal with the unbounded soils. Using the finite/infinite element scheme, Yang and Hung (1997) conducted a parametric investigation on the isolation effect of open trenches, in-filled trenches and elastic foundations. In the last decade, a great portion of the studies on wave propagation problems were performed by the boundary element method, including Beskos *et al.* (1986), Al-Hussaini and Ahmad (1991, 1996), Ahmad *et al.* (1996), among others. One advantage of the boundary element method is that the radiation damping can be accurately taken into account. However, it is not suitable for simulating the realistic situations where irregularities may exist either in the geometry or materials of the structures and underlying soils.

As far as the vibrations of the buildings, foundations, and surrounding soils are concerned, a finite element representation remains the most convenient choice, considering its versatility in treating various irregularities. In the study by Yang *et al.* (1996), it has been demonstrated that radiation damping of the far field can be accurately simulated by the $Q8$ -compatible infinite element they derived. In this study, the same finite/infinite element method will be adopted. To take advantage of both types of elements, the structure and soils in the near field will be modeled by the finite elements, and the radiation property of the far field by the infinite elements. Such an approach is

attractive in that both the finite and infinite elements can be assembled using the conventional procedures, with no additional degrees of freedom required for the far field.

In the literature, most studies concerning wave isolation were focused on reducing the surface vibration. In comparison, relatively few works have been reported on the reduction of building response using open and in-filled trenches. The purpose of this paper is to conduct a parametric study on the open or in-filled trenches for reducing the traffic-induced vibrations on buildings. The soil-structure model considered herein is basically two-dimensional. The building is simulated as a box structure, and the moving train as a harmonic line load. There may exist bedrocks beneath the soils. A parametric study is first conducted for both the open and in-filled trenches in reducing the building vibration at each specific frequency. Then, the screening effect of the trenches over the full range of frequencies considered is examined. Previously, rather few studies have been carried out to evaluate the screening effect of trenches over a wide range of frequencies, due to the diverse requirements existing for the extent and spacing of the finite element grid under different frequencies. However, such a problem can be easily overcome using the self-expansion technique proposed by Yang *et al.* (1996) for the finite/infinite element meshes, by which the far-field impedance matrices for the entire range of frequencies can be derived from the mesh established for the highest frequency considered.

2. Problem formulation and basic assumptions

The soil-structure system considered is shown in Fig. 1, which consists of a near field (Part I) and a semi-infinite far field (Part II). Typically, Part I contains the components that may be irregular in geometry or material, including the building, railway (i.e., source of vibration), wave barriers, and underlying soils, all of which will be represented by the 8-node quadratic (Q8) element in this study. Part II covers the soils in the far field extending to infinity, which will be modeled by the Q8-compatible infinite element to be summarized below. To simulate the action of moving train loads, a line load is applied at the center of the railway. Such an approximation is reasonable provided that the point of interest from the track is approximately less than $1/\pi$ times the length of train (Gutowski and Dym 1976). Moreover, since a general traffic load can always be transformed

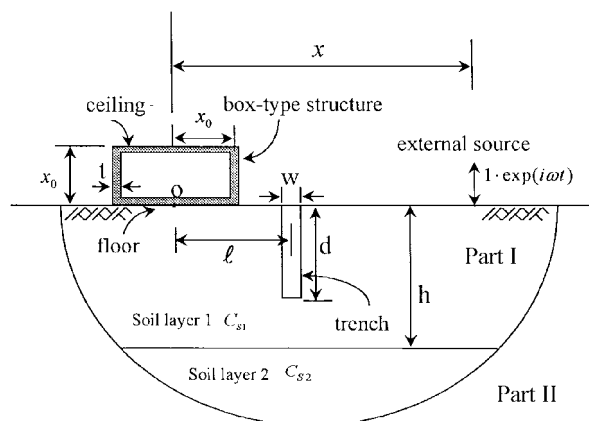


Fig. 1 Typical soil-structure model

into frequency domain and expressed in terms of harmonic functions, only harmonic line loads are considered in this paper. It follows that the displacements generated within the system may be assumed to oscillate harmonically with time as well. Based on the assumption that the length of the building in the direction parallel to the railway is relatively long compared to the width along the direction transverse to the railway, plain strain condition is assumed to apply. The soil is assumed to be an isotropic viscoelastic medium (with hysteresis damping) with or without bedrock.

The formulation of the Q -8 element was well established in the literature, which will not be recapitulated herein. Only the formulation of the Q 8-compatible infinite element to be used in this study will be summarized, based on the works of Yang *et al.* (1996) and Zhang and Zhao (1987). Consider the infinite element in Fig. 2. The following are the transformation for the co-ordinates x and y :

$$x = \sum_{i=1}^5 N_i' x_i \quad y = \sum_{i=1}^5 N_i' y_i \tag{1}$$

where the shape functions N_i' are assumed to be linear in ξ and quadratic in η , i.e.,

$$\begin{aligned} N_1' &= -\frac{1}{2}(\xi - 1)(\eta - 1)\eta \\ N_2' &= (\xi - 1)(\eta - 1)(\eta + 1) \\ N_3' &= -\frac{1}{2}(\xi - 1)(\eta + 1)\eta \\ N_4' &= \frac{1}{2}\xi(\eta + 1) \\ N_5' &= -\frac{1}{2}\xi(\eta - 1) \end{aligned} \tag{2}$$

The element displacements u and v can be interpolated from their nodal values, that is,

$$u = \sum_{i=1}^3 N_i u_i \quad v = \sum_{i=1}^3 N_i v_i \tag{3}$$

where the shape functions are

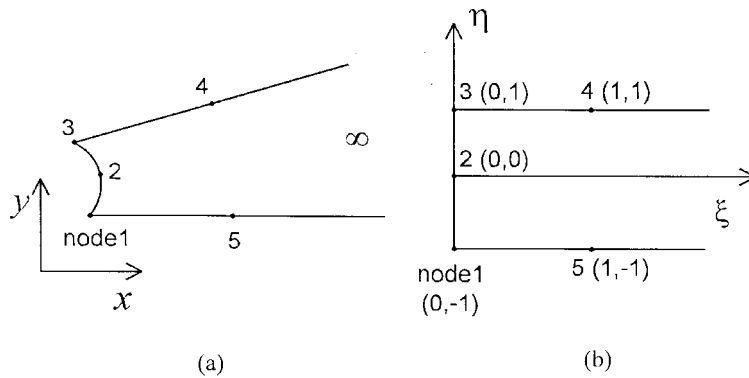


Fig. 2 Infinite element: (a) global co-ordinates; (b) local co-ordinates

$$\begin{aligned}
N_1 &= \frac{1}{2}\eta(\eta - 1)P(\xi) \\
N_2 &= -(\eta - 1)(\eta + 1)P(\xi) \\
N_3 &= \frac{1}{2}\eta(\eta + 1)P(\xi)
\end{aligned} \tag{4}$$

and the propagation function $P(\xi)$ is defined as

$$P(\xi) = \exp(-\alpha_l \xi) \exp(-ik_l \xi) \tag{5}$$

with α_l denoting the displacement amplitude decay factor and k_l the wave number, both in the local co-ordinates. In Eq. (5), the term $\exp(-\alpha_l \xi)$ represents the amplitude attenuation due to wave dispersion and the term $\exp(-ik_l \xi)$ the phase decay due to wave propagation in the direction ξ . The two local parameters α_l and k_l can be related to the parameters k and α in the global co-ordinates as: $\alpha_l = \alpha l$ and $k_l = kl$, where l is the scale factor between the global and local co-ordinates, i.e., $l = x/\xi$. The global parameters are known to be available in practice, if one notes that $k = \omega/c$, where ω and c denote respectively the frequency and velocity of the traveling wave.

According to Yang *et al.* (1996), for the case of a half space subjected to a line load on the free surface, the amplitude decay factor α should be selected as $\alpha = 1/(2R)$ for modeling the regions where the body waves are dominant, where R denotes the distance between the source of vibration and the far field boundary. Since the Rayleigh waves do not decay on the free surface under the same loading condition, it is suggested that $\alpha = 0$ be used for regions near the free surface.

By the finite element procedure of formulation and assuming the loading and displacement functions both to be of the harmonic type, one can derive the equation of motion for the infinite element under a particular exciting frequency ω :

$$-\omega^2 [M] \{\Delta\} + [K] \{\Delta\} = \{F\} \tag{6}$$

where $\{\Delta\}$ and $\{F\}$ denote the amplitude of the nodal displacements and applied loads, respectively. By letting t denote the thickness of the element, the element mass matrix $[M]$ and stiffness matrix $[K]$ can be expressed as

$$[M]_{6 \times 6} = \int_{-1}^1 \int_0^\infty [N]^T [N] t J d\xi d\eta \tag{7}$$

$$[K]_{6 \times 6} = \int_{-1}^1 \int_0^\infty [B]_{6 \times 3}^T [E]_{3 \times 3} [B]_{3 \times 6} t J d\xi d\eta \tag{8}$$

where $[N]$ is the shape function matrix, $[B]$ the strain-displacement matrix, $[E]$ the constitutive matrix and J is the Jacobian of the transformation matrix from the global co-ordinate system to the local co-ordinate system. Conventionally, the term $([K] - \omega^2 [M])$ has been referred to as the impedance matrix, which will be denoted as $[S]$ in this study. Both the matrices $[N]$, $[B]$ and the Jacobian J can be derived from the aforementioned shape functions.

It should be noted that because of the harmonic terms involved in the shape functions, and the unbounded limits of the integrals, i.e., from 0 to ∞ , rather than from -1 to 1 as implied by conventional finite element integrals, the mass and stiffness matrices given in Eqs. (7) and (8) represent one kind of integrals that cannot be evaluated using conventional Gauss integration schemes. To evaluate integrals with directions extending to infinity, i.e., the ξ -direction for the present case, a special integration scheme devised by Bettess and Zienkiewicz (1977) was used.

Other details regarding application of the infinite element presented in this section are available in Yang *et al.* (1996).

3. Scheme for generating finite/infinite element mesh

In this study, the near field including the building will be modeled by the $Q8$ plane elements, and the far field by the $Q8$ -compatible infinite elements. As was stated in Yang *et al.* (1996), the maximum element size and minimum mesh size required depend on the wave length, which in turn depends on the frequency of the problem considered. Hence, for waves of lower frequencies, a finite element mesh of larger extent R should be used. On the contrary, for waves of higher frequencies, an element of smaller size L should be used. The following are the requirements for the finite element mesh in order to achieve accurate results: element size $L \leq \lambda_s/6$ and mesh extent $R \geq 0.5\lambda_s$, where λ_s denotes the shear wave length. Obviously, it is difficult, or at least computationally inefficient, to create a finite/infinite element mesh that can meet the diverse needs of waves of both low and high frequencies. The following is a summary of the procedure for generating the far field impedance matrices for the full range of frequencies using exactly the finite/infinite element mesh established for the highest frequency that is of interest (Yang *et al.* 1996).

Consider the two far fields as indicated by the one with a solid boundary and the other one with a dashed boundary in Fig. 3. Let the two far fields be similar with respect to point O , in the sense that along each radial line originating from point O , the ratio of the distance between point O and the point on the dashed line to the distance between point O and the corresponding point on the solid line remains equal to $n/(n-1)$, where n is an integer, assuming the material properties to be identical along each radial direction. Let $\Delta\omega$ denote a constant frequency increment. It can be ascertained that for the two-dimensional problem, the far field impedance $[S]$ for $\omega=(n-1)\Delta\omega$ at the outer boundary (dashed line) with an extent of $[n/(n-1)]R$ should equal the far field impedance $[S]$ for $\omega=n\Delta\omega$ at the inner boundary (solid line) with a distance of R . In analysis, one may start by calculating the far field impedance $[S]$ for the highest frequency $\omega=n\Delta\omega$ at the inner boundary with distance R , i.e., by assembling the structural impedance matrices of the infinite elements over the inner boundary, and set the far-field impedance $[S]$ for $\omega=(n-1)\Delta\omega$ at the outer boundary with

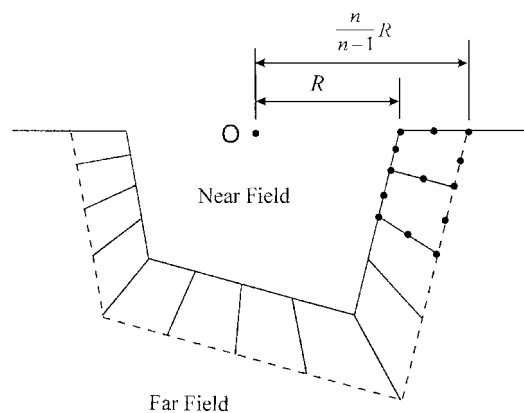


Fig. 3 Schematic of condensation to the inner boundary

distance $[n/(n-1)]R$ equal to it. Then, one can divide the region enclosed by these two boundaries into a number of $Q8$ elements, with the distance between any two adjacent nodes on the outer boundary set equal to $n/(n-1)$ times that of its corresponding distance on the inner boundary. By condensing all the far-field degrees of freedom, including those of the newly inserted $Q8$ elements and those on the outer boundary, to the nodes on the inner boundary, one can obtain the impedance matrix $[S]$ for the next highest frequency $\omega=(n-1)\Delta\omega$ at the inner boundary. The above procedure can be repeated to yield the far-field impedance matrices $[S]$ for all the remaining frequencies $\omega=(n-2)\Delta\omega$, $\omega=(n-3)\Delta\omega$, ..., etc. It should be noted that although the location of the outer boundary moves as the value $(n-1)/n$ changes, such a condensation process can be carried out by internal computer codes. Consequently, only the finite element mesh for the near field need be established prior to analysis, while the rest can be dealt with repetitively by the computer program.

4. Frequency-independent parametric studies

For the purpose of wave reduction, an open or in-filled trench will be constructed between the vibration source and the building to be protected, as shown in Fig. 1. In this section, a homogenous half-space is assumed for the soils underlying the building. The finite/infinite element method described above will be employed to investigate the influence of various parameters upon the screening effect of the open and in-filled trenches at a specific frequency. Based on the criteria stated earlier for mesh generation, a finite/infinite element mesh that meets the present demands was created (Fig. 4). The screening effect of the wave barrier can be evaluated using the amplitude reduction ratio A_r , defined as

$$A_r = \frac{d_a}{d_b} \quad (9)$$

where d_a denotes the average displacement amplitude over the floor (or ceiling) surface of the structure with the wave barrier, and d_b the corresponding average displacement amplitude for the case with no barrier. Obviously, a smaller value of A_r implies that a better effect of isolation has been achieved by the barrier.

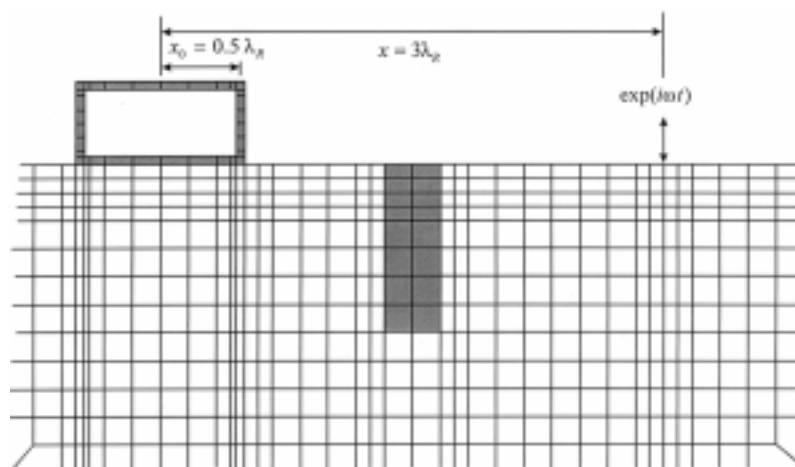


Fig. 4 Finite/infinite element mesh I

Table 1 Material properties of soil-structure model

	Shear modulus G (MPa)	Elastic constant E (MPa)	Poisson's ratio ν	Density ρ (kg/m ³)	Damping ratio β (%)
Soil	43.52	–	0.33	1700	5
In-filled trench	1840	–	0.25	2700	5
Structure	–	21000	0.2	2300	2

In what follows, the influence of geometric and material parameters of the trench, including the width, depth, location, shear modulus and Poisson's ratio, will be discussed. To avoid dependency of the analysis results on the exciting frequency, all the geometric parameters used in this study will be normalized with respect to the Rayleigh wave length λ_R , i.e., $w=W\cdot\lambda_R$, $d=D\cdot\lambda_R$, $l=L\cdot\lambda_R$, $x_0=X_0\cdot\lambda_R$, $t=T\cdot\lambda_R$, $x=X\cdot\lambda_R$ and $h=H\cdot\lambda_R$, where the parameters W , D , L , X_0 , T , X and H are dimensionless. Unless otherwise noted, $D=1$ and $L=3/2$ will be adopted exclusively for both the open and in-filled trenches, and $W=1/3$ and $W=1/2$ for the open and in-filled trench, respectively. In the parametric study, the soil and building properties, as well as the location for the external load, will be kept constant, i.e., $X_0=1/2$, $T=1/20$ and $X=3$ will be adopted throughout the analysis and the soil extending to infinity ($H\rightarrow\infty$) is assumed to be homogeneous, viscoelastic. All the material properties assumed for the standard case have been listed in Table 1. Using the present data, the shear wave velocity C_s for the soil is 160 m/s, and the Rayleigh wave velocity is 150 m/s.

4.1 Normalized distance (L) between the structure and open trench

The results computed for the ceiling and floor of the structure by varying the distance L between the structure and the trench have been plotted in Fig. 5. As can be seen, the difference between the ceiling and floor responses with regard to the effect of isolation is not noticeable. For both the ceiling and floor responses, it can be observed that the isolation efficiency of the trench decreases when it is located either close to the source (i.e., with $L=2.5$) or close to the structure (i.e., with $L=0.75$). One possible reason for this is that at places near the external source, the body waves play a role more important than the surface waves. Since the body waves decay slowly downward from the surface, a great portion of these waves can pass through below the trench as it is located close to the source, thereby reducing the effect of screening. On the other hand, as the open trench is located near the building, because of the unstable nature of the open trench, it will cause the neighboring building to vibrate and thus reduce the effect of isolation.

4.2 Normalized depth (D) and width (W) of the open trench

By changing the depth (D) of the open trench, the results computed for the vertical response of the floor of the structure have been plotted against the normalized width (W) in Fig. 6. It can be observed that for shallow trenches, say, with $D=1/3$ and $D=2/3$, the wider the trench, the worse the effect of isolation is. In contrast, for deep trenches, greater width may result in better screening effect, although the phenomenon is only marginal. One reason for this is that as D is small, the use of wider trenches, which means wider free surface, allows the body waves to be transformed into the surface waves, which suffer little geometric attenuation in traveling. As a consequence, the influence of width becomes pronounced. Besides, the figure indicates that for $D \geq 1$, the influence

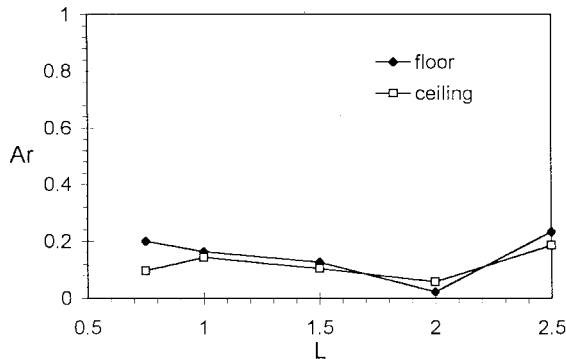


Fig. 5 Effect of normalized distance from structure to open trench

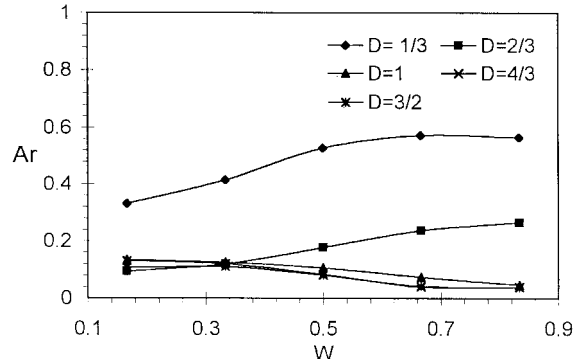


Fig. 6 Effect of normalized (open) trench depth and width on floor response

of the trench depth becomes rather minor. However, for small D values, say, for $D \leq 2/3$, an increase in the trench depth can improve significantly the effect of isolation. It should be added that a trend similar to the one given in Fig. 6 exists for the ceiling, which is not shown here for brevity.

4.3 Normalized distance (L) between the building and in-filled trench

The amplitude reduction ratios A_r for both the ceiling and floor of the building have been plotted against the distance L between the building and in-filled trench in Fig. 7. From this figure, a trend opposite to that of the open trench is observed, that is, the screening effect appears to be greater when the in-filled trench is located either close to the source (with $L=2.5$) or to the building (with $L=0.75$). It is hard to explain why the in-filled trench shows better isolation effect when located closer to the source, i.e., with $L=2.5$, due to the complex nature of the wave propagation phenomenon, which may involve reflection, refraction, diffraction, mode conversion of waves and soil-structure interaction. Nevertheless, it is natural to see that the in-filled trench performs better when located closer to the building, as it is stiffer than the nearby soils, which tends to constrain the adjoining building from vibration.

4.4 Normalized depth (D) and width (W) of the in-filled trench

To investigate the effect of the trench dimensions in reducing the floor response of the structure, the influence of the trench width W is investigated for different values of the trench depth D . As can be seen from Fig. 8, the deeper the trench, the better the isolation effect is. This figure also reveals that for shallow trenches, say, with $D \leq 2/3$, an increase in the trench width does not always lead to better isolation. The result for the ceiling response is similar to the one given in Fig. 8 for the floor response, which is not shown here.

4.5 Impedance ratio (IR) of the in-filled trench

The impedance ratio (IR) is a factor widely used by geotechnic engineers to distinguish whether a wave barrier is soft or hard with respect to the surrounding soil, which is defined as

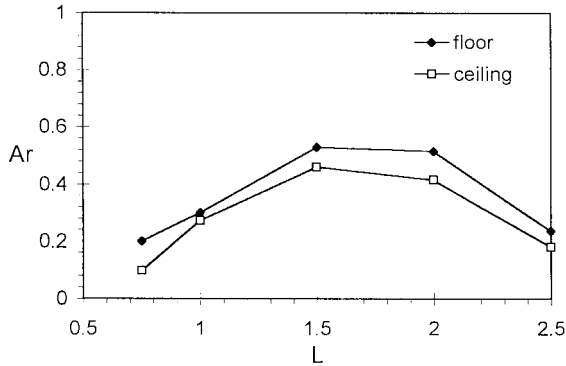


Fig. 7 Effect of normalized distance from structure to in-filled trench

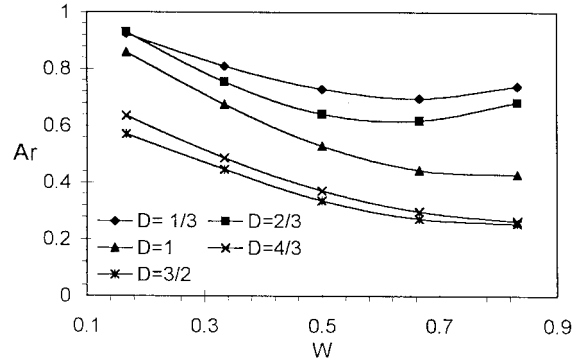


Fig. 8 Effect of normalized (in-filled) trench depth and width on floor response

$$IR = \frac{\rho_b V_b}{\rho_s V_s} \tag{10}$$

where ρ_b and ρ_s denote the mass density of the barrier and the soil, respectively, and V_b and V_s the shear wave velocities of the two. Since the shear wave velocity V can be related to the shear modulus and mass density, i.e., $V=(G/\rho)$, the preceding equation can be rewritten,

$$IR = \sqrt{\frac{\rho_b G_b}{\rho_s G_s}} \tag{11}$$

where G_b and G_s denote the shear modulus of the in-filled trench and the underlying soil, respectively. In this section, only the shear modulus G_b of the in-filled trench is allowed to vary, while the shear modulus G_s of the soil and the mass densities for both the trench and soil will be kept constant.

The amplitude reduction ratio A_r has been plotted against the impedance ratio IR for both the ceiling and floor responses in Fig. 9. As can be seen from the right-hand part of the figure, the increasing of IR can result in better isolation effect for trenches that are stiffer than the soil, i.e., for trenches with $IR > 1$. However, the amplitude reduction ratio A_r tends to approach a limit value of 0.5 and 0.45 for the floor and the ceiling, respectively, as the barrier gets harder. Generally, the use of $IR = 7$ can be regarded as an optimal choice for hard barriers. On the other hand, from the left-hand part of Fig. 9, it can be observed that for barriers that are softer than the soil, i.e., for trenches with $IR < 1$, the amplitude reduction ratio A_r declines dramatically as the impedance ratio IR becomes smaller and reaches a minimum of 0.05 when $IR = 0.11$. A scrutiny of this figure reveals that as the impedance ratio IR approaches zero, the amplitude reduction ratio A_r will approach the value given in Fig. 6 for the open trench with $W = 1/2$ and $D = 1$. Such a phenomenon can be easily conceived since the open trench is nothing but a special case of the in-filled trench with $IR = 0$. From the point of construction, an in-filled trench with $IR < 1$ can be achieved using properly designed soil-bentonite mix as the fill material.

4.6 Poisson's ratios (ν_b, ν_s)

The variation in the reduction ratio for the floor response over different Poisson's ratios of the trench (ν_b) and the underling soil (ν_s) has been plotted in Fig. 10, in which the results for $\nu_s=0.25$,

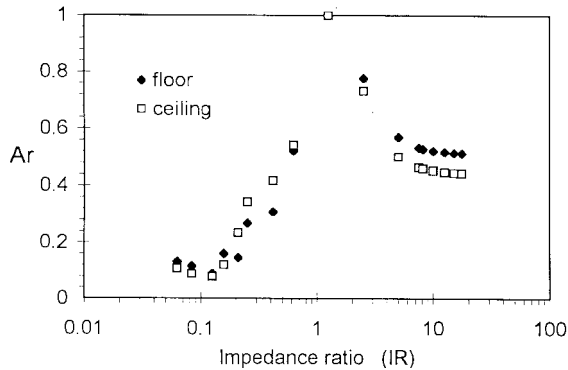


Fig. 9 Effect of impedance ratio for in-filled trench

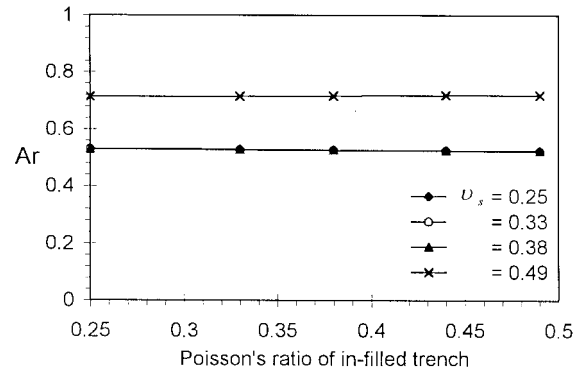


Fig. 10 Effect of Poisson's ratio for in-filled trench

0.33, 0.38 are almost coincident. As can be seen, an increase in the Poisson ratio ν_s of the soil from 0.25 to 0.38 causes basically no difference on the isolation response. However, as the Poisson ratio ν_s of the soil equals 0.49, drastic decline on the isolation effect may occur. Such a phenomenon can be attributed to the distinct influence of the Poisson ratio of the soil on the compressional wave velocity C_p and, accordingly, on the wave length. The compressional wave velocity C_p can be related to the shear wave velocity C_s as: $C_p = \sqrt{2(1 - \nu_s)/(1 + 2\nu_s)} C_s$. As the Poisson ratio ν_s change from 0.25 to 0.38, the compressional wave length increases by 1.31 times, while as the Poisson's ratio ν_s changes from 0.25 to 0.49, the compressional wave length increases by more than 4 times. Hence, for the case with $\nu_s=0.49$, deeper trenches are required to achieve the same degree of isolation. Besides, the figure indicates that changing ν_s causes basically no influence on the isolation response. The above observations remain valid for the isolation of ceiling response, which are not shown here. As a side note, the influence of the damping ratio and mass density of the soil on isolation of building response is not significant for practical applications, which is also omitted.

5. Effect of frequencies and soil conditions

In the preceding parametric studies, all the results obtained are independent of the exciting frequency of the driving force because all the geometric parameters have been normalized with respect to the Rayleigh wave length. However, as the traffic loads cover a wide range of frequencies and the building size x_0 remains fixed in practice, the parametric studies conducted in the preceding section under the assumption that the half-width of the building equals half of the Rayleigh wave length ($x_0=1/2\lambda_R$) appear to be insufficient or meaningless for the purpose of engineering applications. In this section, the screening effect of the open and in-filled trenches will be investigated in a more realistic manner under the range of frequencies considered for different soil conditions. The model adopted in this section is exactly identical to the one given in Fig. 1. For the present case, however, all the geometric parameters will be normalized respect to the half-width x_0 of the building, rather than the Rayleigh wave length λ_R . In particular, the thickness of the building is assumed to be $t = 1/10 x_0$, the location of vibration source is $x = 4.5 x_0$ and the depth of soil layer 1 is $h = 2 x_0$. For the open trench, the depth and width are $d = 1.5 x_0$, $w = 0.25 x_0$, and the distance from the trench to the building center is $l = 1.25 x_0$. And for the in-filled trench, the following data are used: $d = 1.5 x_0$, $w = 0.5 x_0$, and $l = 1.25 x_0$. All the material properties for soil layer 1, as well as those for the

structure and the trench, are the same as those listed in Table 1. For the present purposes, two different conditions will be considered for the soils. One is a homogeneous half-space soil with no bedrock, which can be achieved by setting the shear wave velocity of layer 2 equal to layer 1, i.e., $C_{s2} = C_{s1} = 160$ m/s. The other is a soil supported by bedrock, which can be achieved by assigning a rather high value to the shear wave velocity of layer 2, say, using $C_{s2} = 1200$ m/s. Through a careful examination of the present data for the soil and structure, a finite/infinite element mesh was created as shown in Fig. 11.

The non-dimensional frequency factor $\omega x_0/C_s$ is used as a frequency parameter, where ω denotes the exciting frequency and C_s the shear wave velocity of soil layer 1. The average response of both the ceiling and floor of the structure will be analyzed. In addition to the normalized vertical response V/G , where V denotes the vertical displacement and G the shear modulus of soil layer 1, a log-scale vibration acceleration level (VAL) with the unit dB will also be adopted to present the analysis results,

$$\text{relative VAL[dB]} = 20 \log_{10} \frac{\text{calculated acceleration}}{\text{reference acceleration}} \quad (12)$$

where the reference acceleration is obtained from the response of a reference analysis in which no trench is present. Obviously, the relative VAL serves as an indicator of the effectiveness of the trench in reducing the building vibrations.

5.1 Soil with no bedrock

Figs. 12(a) and (b) respectively depict the vertical response of the ceiling and the floor under different frequencies. As can be seen, the resonance responses occur at $\omega x_0/C_s = 0.6$ and 1.1 for the ceiling, but no resonance response occurs on the floor. The non-consistence in the response of the ceiling and floor can be attributed to the fact that the floor is in direct contact with the soil, but the ceiling is not. Consequently, the resonance frequencies occurring on the ceiling should be interpreted as the natural frequencies of the building.

Corresponding to Figs. 12(a) and (b), the effectiveness of the trenches in reducing the ceiling and

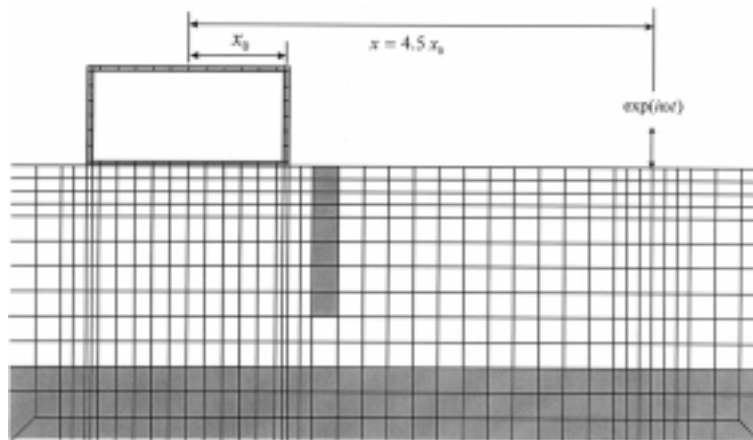


Fig. 11 Finite/infinite element mesh II

floor responses has been plotted in terms of the relative VAL in Figs. 13(a) and (b), respectively. From these figures, it is clear that although the trenches are very helpful for reducing the high-frequency vibrations, basically no isolation effect can be achieved at lower frequencies, say, in the range with $\omega x_0 / C_s < 1.3$ for the ceiling and with $\omega x_0 / C_s < 1.0$ for the floor. Such a result can be easily interpreted using the relation: $\lambda = 2\pi C / \omega$, where λ is the wave length and C the wave velocity. As the soil properties remain unchanged, so does the wave velocity C . It follows that a lower frequency ω implies a longer wave length λ . Hence, to achieve the same level of isolation, deeper trenches must be used for waves of lower frequencies, because of their longer wave lengths. However, as was shown in Fig. 12, the response of the building for the case without bedrock are dominated by lower frequencies. Thus, if one is interested in mitigating the low-frequency response for the present case, the trenches should not be regarded as a proper tool. Besides, the results also demonstrate that the open trench tends to isolate the vibration more effectively than the in-filled trench, and that there is no monotonous increase of the screening effect with relation to increase of the frequency, especially for the open trench. This implies that for a specific frequency, an increase of the trench dimension does not always lead to better isolation effect, which is consistent with the observations made in the preceding section.

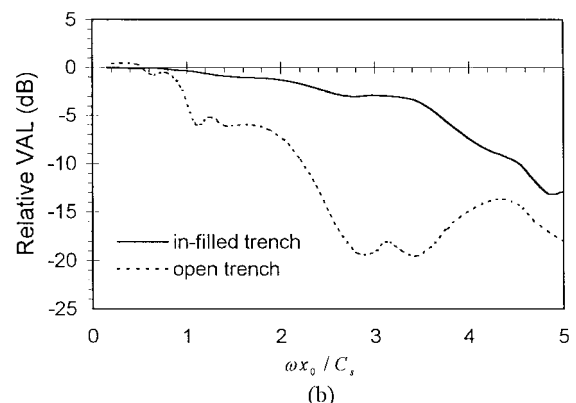
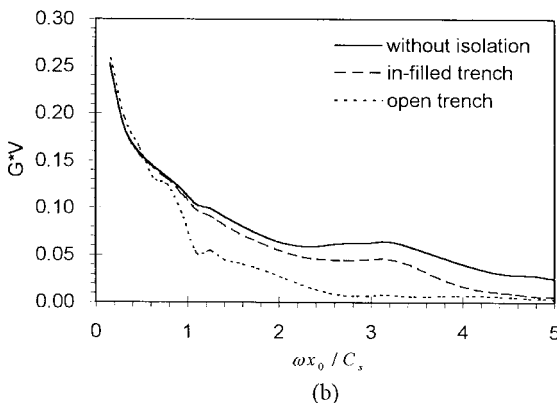
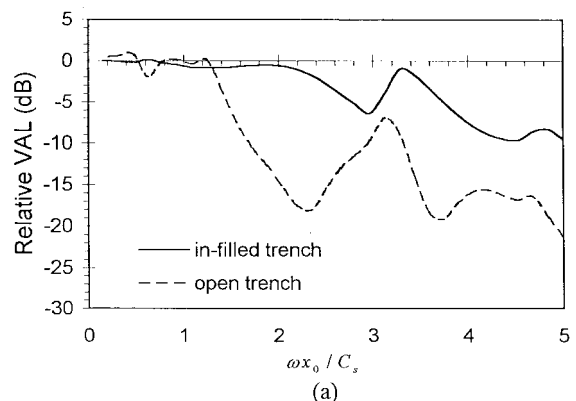
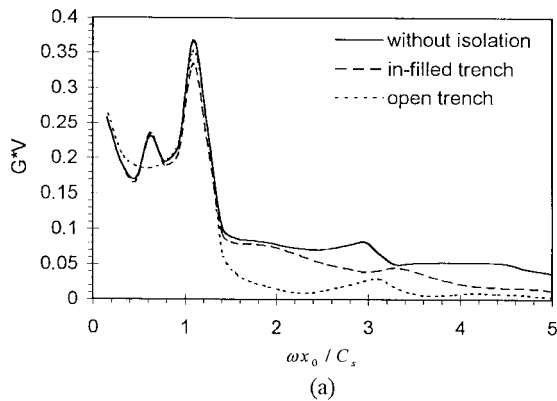


Fig. 12 Effect of frequency for soil without bedrock on vertical displacement of (a) ceiling, (b) floor

Fig. 13 Effect of frequency for soil without bedrock on VAL response of (a) ceiling, (b) floor

5.2 Soil with bedrock

To simulate the effect of underlying bedrock, the shear wave velocity of soil layer 2 is assumed to be eight times that of layer 1. The absolute values of the vertical displacement of the ceiling and floor of the building versus the non-dimensional frequency factor have been plotted in Figs. 14(a) and (b), respectively. By comparing the results for the present case with those for the case with no bedrock in Fig. 12, one observes that pretty low responses occur at lower frequencies for the case with bedrock. This can be attributed to the fact that no vibration eigenmodes can be induced below the cutoff frequency of the soil stratum. According to Wolf (1985), the cutoff frequency is $C_p/(4h)$ (equivalent to $\omega x_0/C_s = \pi/4(C_p/C_s) = 1.56$) for the vertical injected compressional wave and is $C_s/(4h)$ (equivalent to $\omega x_0/C_s = \pi/4 = 0.79$) for the shear wave. Another observation is that, unlike the case with no bedrock, the floor may become in resonance with the soil stratum, with rather large peak response induced. Here, the resonance frequency of the soil stratum is $(2n-1)C_p/(4h) = (2n-1)1.56 = 1.56, 4.68, \dots$, for the compressional waves, and $(2n-1)C_s/(4h) = (2n-1)0.79 = 0.79, 2.36, \dots$, for the shear waves.

Corresponding to Figs. 14(a) and (b), the effectiveness of the trenches in reducing the ceiling and floor response has been plotted in terms of the relative VAL in Figs. 15(a) and (b), respectively. A

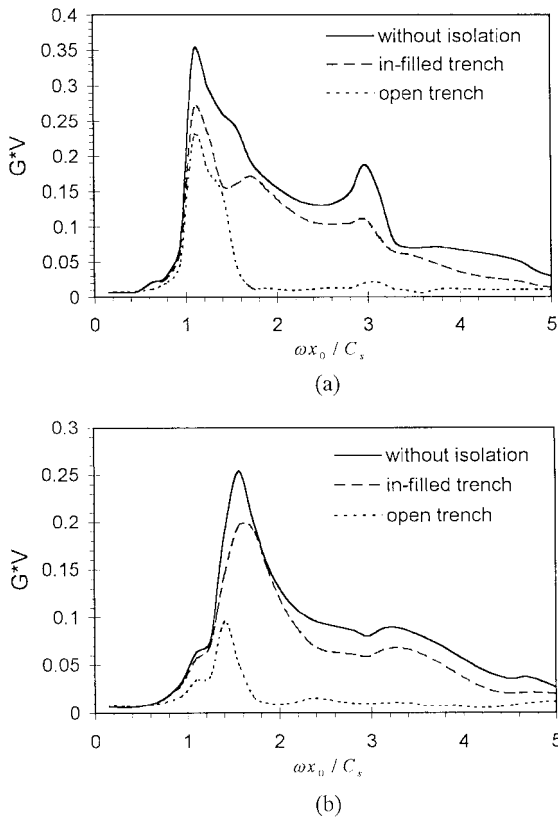


Fig. 14 Effect of frequency for soil with bedrock on vertical response of (a) ceiling, (b) floor

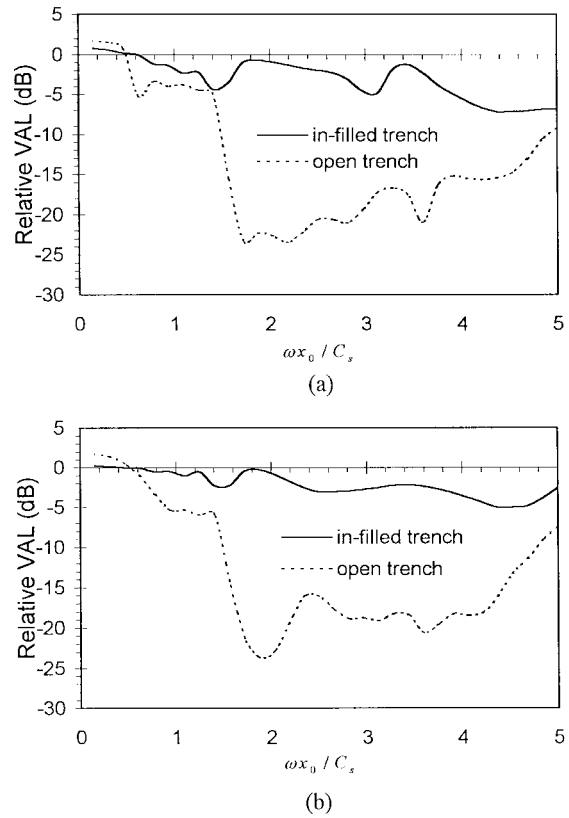


Fig. 15 Effect of frequency for soil with bedrock on VAL response of (a) ceiling, (b) floor

comparison of these figures with those for the case with no bedrock (Fig. 13) indicates that similar trend exists between these two, implying that the existence of the bedrock causes basically no difference to the efficiency of isolation of the trenches. However, as was revealed by Fig. 14, the building response becomes rather small at lower frequencies due to presence of the bedrock. Thus, the potential drawback of the trenches in reducing the low-frequency response becomes insignificant for the case with bedrock.

6. Conclusions

The following conclusions can be drawn from the results presented in this paper: (1) In order to achieve a good effect of isolation, the open or in-filled trenches should have a depth of the same order as that of the Rayleigh wave length. As a result, the isolation of ground-borne vibrations by trenches is effective only for moderate to high frequency vibrations. (2) The open trench tends to perform better than the in-filled trench for the cases studied. However, the open trench is inferior to the in-filled trench because of its higher difficulty in construction and higher cost of maintenance. (3) Soils with large Poisson's ratios can reduce the effect of isolation brought by the trenches, since they can increase considerably the compressional wavelength. (4) The stiffer (or softer) an in-filled trench with respect to the surrounding soil, the better the effect of isolation is. (5) Although the ceiling response differs significantly from the floor response due to involvement of the building frequencies, the efficiency of trenches in isolating the ceiling and floor responses appears to be similar. (6) For soils with bedrock, the response of the building at frequencies lower than the cutoff frequencies becomes rather small, as compared with the case without bedrock. However, the response may become more pronounced at frequencies equal to or higher than the cutoff frequency because of the resonance effect of the soil stratum. Both the cutoff effect and the resonance effect should be considered if an artificial bedrock is to be installed at a certain depth under the structure or the source to mitigate the train-induced vibrations.

Acknowledgments

The research reported herein was sponsored in part by the National Science Council through Grant No. NSC 88-2211-E-002-017. The paper has been rewritten from the one presented at the *1st International Conference on Advances in Structural Engineering and Mechanics*, August 23-25, 1999, Seoul, Korea.

References

- Ahmad, S., Al-Hussaini, T.M., and Fishman, K.L. (1996), "Investigation on active isolation of machine foundations by open trench", *J. Geotech. Eng., ASCE*, **122**(6), 454-461.
- Alabi, B. (1992), "A parametric study on some aspects of ground-borne vibrations due to rail traffic", *J. Sound Vib.*, **153**(1), 77-87.
- Al-Hussaini, T.M., and Ahmad, S. (1991), "Design of wave barriers for reduction of horizontal ground vibration", *J. Geotech. Eng., ASCE*, **117**(4), 616-636.
- Al-Hussaini, T.M., and Ahmad, S. (1996), "Active isolation of machine foundations by in-filled trench barriers",

- J. Geotech. Eng.*, ASCE, **122**(4), 288-294.
- Antes, H., and von Estorff, O. (1994), "Dynamic response of 2D and 3D block foundations on a halfspace with inclusions", *Soil Dyn. Earthq. Eng.*, **13**, 305-311.
- Balendra, T., Chua, K.H., Lo, K.W., and Lee, S.L. (1989), "Steady-state vibration of subway-soil-building system", *J. Eng. Mech.*, ASCE, **115**(1), 145-162.
- Beskos, D.E., Dasgupta, B., and Vardoulakis, I.G. (1986), "Vibration isolation using open or filled trenches", *Comput. Mech.*, **1**, 43-63.
- Bettess, P., and Zienkiewicz, O.C. (1977), "Diffraction and refraction of surface waves using finite and infinite elements", *Int. J. Numer. Meth. Eng.*, **11**, 1271-1290.
- Boroomand, B., and Kaynia, A.M. (1991), "Vibration isolation by an array of piles", *Soil Dyn. Earthq. Eng.*, **11**, 684-691.
- Dawn, T.M., and Stanworth, C.G. (1979), "Ground vibration from passing trains" *J. Sound Vib.*, **66**(3), 355-362.
- Emad, K., and Manolis, G.D. (1985), "Shallow trench and propagation of surface waves", *J. Eng. Mech.*, ASCE, **111**(2), 279-282.
- Grootenhuis, P. (1977), "Floating track slab isolation for railway", *J. Sound Vib.*, **51**(3), 443-448.
- Gutowski, T.G., and Dym, C.L. (1976), "Propagation of ground vibration: A review", *J. Sound Vib.*, **49**(2), 179-193.
- Heckl, M., Hauck, G., and Wetschurck, R. (1996), "Structure-borne sound and vibration from rail traffic", *J. Sound Vib.*, **193**(1), 175-184.
- Krylov, V., and Ferguson, C. (1994), "Calculation of low-frequency ground vibration from railway train", *Appl. Acoust.*, **42**, 199-213.
- Krylov, V. (1995), "Generation of ground vibrations by superfast trains", *Appl. Acoust.*, **44**, 149-164.
- Lysmer, J., and Wass, G. (1972), "Shear waves in plane infinite structures", *J. Eng. Mech. Div.*, ASCE, **98**(EM1), 85-105.
- Madshus, C., Bessason, B., and Harvik, L. (1996), "Prediction model for low frequency vibration from high speed railways on soft ground", *J. Sound Vib.*, **193**(1), 195-203.
- Schmid, G., Chouw, N., and Le, R. (1991), "Shielding of structure from soil vibration", *Soil Dyn. Earthq. Eng.*, **11**, 651-662.
- Segol, G., Lee, C.Y., and Abel, J.F. (1978), "Amplitude reduction of surface waves by trenches", *J. Eng. Mech. Div.*, ASCE, **104**(EM3), 621-641.
- Takahashi, D. (1985), "Wave propagation in ground-structure systems with line contact", *J. Sound Vib.*, **101**(4), 523-537.
- Takahashi, D. (1986a), "Wave propagation in ground-structure systems. Part I: Analysis of the model with surface contact", *J. Sound Vib.*, **105**(1), 27-36.
- Takahashi, D. (1986b), "Wave propagation in ground-structure systems. Part II: Parametric survey", *J. Sound Vib.*, **105**(1), 37-48.
- Wilson, G.P., Saurenman, H.J., and Nelson, J.T. (1983), "Control of ground-borne vibration noise and vibration", *J. Sound Vib.*, **87**(2), 339-350.
- Wolf, J.P. (1985), *Dynamic Soil-Structure Interaction*, Prentice-Hall, Englewood Cliffs, New Jersey, 292-293.
- Woods, R.D. (1968), "Screening of surface wave in soils", *J. Soil Mech. Found. Div.*, ASCE, **94**, 951-979.
- Yang, Y.B., Kuo, S.R., and Hung, H.H. (1996), "Frequency-independent infinite elements for analysing semi-infinite problems", *Int. J. Numer. Meth. Eng.*, **39**, 3553-3569.
- Yang, Y.B., and Hung, H.H. (1997), "A parametric study of wave barriers for reduction of train-induced vibrations", *Int. J. Numer. Meth. Eng.*, **40**, 3729-3747.
- Yang, S.C., and Yun, C.B. (1992), "Axisymmetric infinite elements for soil-structure interaction analysis", *Eng. Struct.*, **14**(6), 361-370.
- Yun, C.B., and Kim, J.M. (1995), "Axisymmetric elastodynamic infinite elements for multi-layered half-space", *Int. J. Numer. Meth. Eng.*, **38**, 3723-3743.
- Zhang, C., and Zhao, C. (1987), "Coupling method of finite and infinite elements for strip foundation wave problems", *Earthq. Eng. Struct. Dyn.*, **15**, 839-851.